

effects may be attributed to activation of several paracrine molecules, rather than a single molecule. Although some may argue what kinds of cytokines play a major role in generating therapeutic effects among the many complex molecular and cellular mechanisms involved, we consider that establishment of mature vessels is a complex process that is not regulated by specific factors, but rather numerous multiple factors that also dynamically change in response to the process of angiogenesis or vessel maturation. We believe that use of a cell-sheet and pedicle-OM as synergistic intelligent engineered tissues can efficiently support the regenerative process by dynamic cross-talk with ischemic cardiac tissue.

Although we did not experience any complication such as torsion of omentum flap or diaphragmatic hernia in the rats receiving the combined treatment, it is considered that a conventional laparotomy itself may adversely affect general conditions particularly in critically-ill heart failure patients. An endoscopic approach may be useful in minimizing the OM-flap procedure-related complications in clinical settings.

## CONCLUSION

We demonstrated that cell-sheet transplantation with an omentum-flap better promoted arteriogenesis and improved coronary microcirculation physiology in ischemic myocardium tissue, leading to potent functional recovery in a rat MI model. Further development of this treatment strategy toward clinical application is encouraged.

## MATERIALS AND METHODS

All experimental procedures were approved by an institutional ethics committee. Animal care was conducted humanely in compliance with the Principles of Laboratory Animal Care formulated by the National Society for Medical Research and the Guide for the Care and Use of Laboratory Animals, prepared by the Institute of Animal Resources and published by the National Institutes of Health (publication no. 85-23, revised 1996).

Two weeks after left coronary artery ligation, rats were divided into four groups: (i) skeletal myoblast cell-sheet transplantation covered with an OM-flap (combined group), (ii) cell-sheet transplantation only, (iii) OM-flap only, and (iv) sham operation (control group). The protocol of this study is shown in **Figure 1a,b**. All *in vivo* and *in vitro* assessments were carried out in a blinded manner. A detailed description of all methods and reagents used for the experiments is provided in the **Supplementary Materials and Methods**.

## SUPPLEMENTARY MATERIAL

Figure S1. Frequency distribution charts showing individual segment caliber changes in response to acetylcholine in **(a)** third and **(b)** fourth branching order vessels. Materials and Methods.

## ACKNOWLEDGMENTS

We thank Tsuyoshi Ishikawa, Yuuka Fujiwara, Yuka Kataoka, Hiromi Nishinaka, Toshika Senba, and staff of the PET Molecular Imaging Center for their excellent technical assistance. This research was supported by Research on Regenerative Medicine for Clinical Application from the Ministry of Health, Labour and Welfare of Japan and the Australian Synchrotron International Synchrotron Access Program (ISAP AS-IA111). Experiments were performed at the Japan Synchrotron Radiation Research Institute (SPring-8, BL28B2, Proposal 2011A1169). T.S. is a consultant for CellSeed, Inc., and T.O. is an Advisory Board Member of CellSeed, Inc. and an inventor/developer holding a patent for temperature-responsive culture surfaces. The authors have no conflicts of interest to report.

## REFERENCES

- Shah, AM and Mann, DL (2011). In search of new therapeutic targets and strategies for heart failure: recent advances in basic science. *Lancet* **378**: 704–712.
- Narita, T, Shintani, Y, Ikebe, C, Kaneko, M, Harada, N, Tshuma, N *et al.* (2013). The use of cell-sheet technique eliminates arrhythmogenicity of skeletal myoblast-based therapy to the heart with enhanced therapeutic effects. *Int J Cardiol* **168**: 261–269.
- Sekiya, N, Matsumiya, G, Miyagawa, S, Saito, A, Shimizu, T, Okano, T *et al.* (2009). Layered implantation of myoblast sheets attenuates adverse cardiac remodeling of the infarcted heart. *J Thorac Cardiovasc Surg* **138**: 985–993.
- Habib, GB, Heibig, J, Forman, SA, Brown, BG, Roberts, R, Terrin, ML *et al.* (1991). Influence of coronary collateral vessels on myocardial infarct size in humans. Results of phase I thrombolysis in myocardial infarction (TIMI) trial. The TIMI Investigators. *Circulation* **83**: 739–746.
- Carmeliet, P and Jain, RK (2011). Molecular mechanisms and clinical applications of angiogenesis. *Nature* **473**: 298–307.
- Gutiérrez, E, Flammer, AJ, Lerman, LO, Elízaga, J, Lerman, A and Fernández-Avilés, F (2013). Endothelial dysfunction over the course of coronary artery disease. *Eur Heart J* **34**: 3175–3181.
- Shirai, M, Schwenke, DO, Tsuchimochi, H, Umetani, K, Yagi, N and Pearson, JT (2013). Synchrotron radiation imaging for advancing our understanding of cardiovascular function. *Circ Res* **112**: 209–221.
- Furchgott, RF and Zawadzki, JV (1980). The obligatory role of endothelial cells in the relaxation of arterial smooth muscle by acetylcholine. *Nature* **288**: 373–376.
- Banquet, S, Gomez, E, Nicol, L, Edwards-Lévy, F, Henry, JP, Cao, R *et al.* (2011). Arteriogenic therapy by intramyocardial sustained delivery of a novel growth factor combination prevents chronic heart failure. *Circulation* **124**: 1059–1069.
- O'Shaughnessy, L (1937). Surgical treatment of cardiac ischemia. *Lancet* **232**: 185–194.
- Takaba, K, Jiang, C, Nemoto, S, Saji, Y, Ikeda, T, Urayama, S *et al.* (2006). A combination of omental flap and growth factor therapy induces arteriogenesis and increases myocardial perfusion in chronic myocardial ischemia: evolving concept of biologic coronary artery bypass grafting. *J Thorac Cardiovasc Surg* **132**: 891–899.
- Shrager, JB, Wain, JC, Wright, CD, Donahue, DM, Vlahakes, GJ, Moncure, AC *et al.* (2003). Omentum is highly effective in the management of complex cardiothoracic surgical problems. *J Thorac Cardiovasc Surg* **125**: 526–532.
- Shudo, Y, Miyagawa, S, Fukushima, S, Saito, A, Shimizu, T, Okano, T *et al.* (2011). Novel regenerative therapy using cell-sheet covered with omentum flap delivers a huge number of cells in a porcine myocardial infarction model. *J Thorac Cardiovasc Surg* **142**: 1188–1196.
- Kawamura, M, Miyagawa, S, Fukushima, S, Saito, A, Miki, K, Ito, E *et al.* (2013). Enhanced survival of transplanted human induced pluripotent stem cell-derived cardiomyocytes by the combination of cell sheets with the pedicled omental flap technique in a porcine heart. *Circulation* **128**(11 Suppl 1): S87–S94.
- Mancuso, MR, Davis, R, Norberg, SM, O'Brien, S, Sennino, B, Nakahara, T *et al.* (2006). Rapid vascular regrowth in tumors after reversal of VEGF inhibition. *J Clin Invest* **116**: 2610–2621.
- Inai, T, Mancuso, M, Hashizume, H, Baffert, F, Haskell, A, Baluk, P *et al.* (2004). Inhibition of vascular endothelial growth factor (VEGF) signaling in cancer causes loss of endothelial fenestrations, regression of tumor vessels, and appearance of basement membrane ghosts. *Am J Pathol* **165**: 35–52.
- Shimizu, T, Sekine, H, Yang, J, Isoi, Y, Yamato, M, Kikuchi, A *et al.* (2006). Polysurgery of cell sheet grafts overcomes diffusion limits to produce thick, vascularized myocardial tissues. *FASEB J* **20**: 708–710.
- Carmeliet, P and Conway, EM (2001). Growing better blood vessels. *Nat Biotechnol* **19**: 1019–1020.
- Hagège, AA, Vilquin, JT, Bruneval, P and Menasché, P (2001). Regeneration of the myocardium: a new role in the treatment of ischemic heart disease? *Hypertension* **38**: 1413–1415.
- Weis, SM and Cheresch, DA (2005). Pathophysiological consequences of VEGF-induced vascular permeability. *Nature* **437**: 497–504.
- Cao, Y, Hong, A, Schulten, H and Post, MJ (2005). Update on therapeutic neovascularization. *Cardiovasc Res* **65**: 639–648.
- Adams, RH and Alitalo, K (2007). Molecular regulation of angiogenesis and lymphangiogenesis. *Nat Rev Mol Cell Biol* **8**: 464–478.
- Jenkins, MJ, Edgley, AJ, Sonobe, T, Umetani, K, Schwenke, DO, Fujii, Y *et al.* (2012). Dynamic synchrotron imaging of diabetic rat coronary microcirculation *in vivo*. *Arterioscler Thromb Vasc Biol* **32**: 370–377.
- Iwasaki, H, Fukushima, K, Kawamoto, A, Umetani, K, Oyama, A, Hayashi, S *et al.* (2007). Synchrotron radiation coronary microangiography for morphometric and physiological evaluation of myocardial neovascularization induced by endothelial progenitor cell transplantation. *Arterioscler Thromb Vasc Biol* **27**: 1326–1333.
- Ludmer, PL, Selwyn, AP, Shook, TL, Wayne, RR, Mudge, GH, Alexander, RW *et al.* (1986). Paradoxical vasoconstriction induced by acetylcholine in atherosclerotic coronary arteries. *N Engl J Med* **315**: 1046–1051.
- Marti, CN, Gheorghade, M, Kalođeropoulos, AP, Georgiopolou, VV, Quyyumi, AA and Butler, J (2012). Endothelial dysfunction, arterial stiffness, and heart failure. *J Am Coll Cardiol* **60**: 1455–1469.
- Bonetti, PO, Lerman, LO and Lerman, A (2003). Endothelial dysfunction: a marker of atherosclerotic risk. *Arterioscler Thromb Vasc Biol* **23**: 168–175.
- Poelzl, G, Frick, M, Huegel, H, Lackner, R, Alber, HF, Mair, J *et al.* (2005). Chronic heart failure is associated with vascular remodeling of the brachial artery. *Eur J Heart Fail* **7**: 43–48.
- Meyer, B, Mörtl, D, Strecker, K, Hülsmann, M, Kulemann, V, Neunteufl, T *et al.* (2005). Flow-mediated vasodilation predicts outcome in patients with chronic heart failure: comparison with B-type natriuretic peptide. *J Am Coll Cardiol* **46**: 1011–1018.
- Heitzer, T, Baldus, S, von Kodolitsch, Y, Rudolph, V and Meinertz, T (2005). Systemic endothelial dysfunction as an early predictor of adverse outcome in heart failure. *Arterioscler Thromb Vasc Biol* **25**: 1174–1179.





## Targeted Delivery of Adipocytokines Into the Heart by Induced Adipocyte Cell-Sheet Transplantation Yields Immune Tolerance and Functional Recovery in Autoimmune-Associated Myocarditis in Rats

Sokichi Kamata, MD, PhD; Shigeru Miyagawa, MD, PhD; Satsuki Fukushima, MD, PhD;  
Yukiko Imanishi, PhD; Atsuhiko Saito, PhD; Norikazu Maeda, MD, PhD;  
Iichiro Shimomura, MD, PhD; Yoshiki Sawa, MD, PhD

**Background:** Clinical prognosis is critically poor in fulminant myocarditis, while its initiation or progression is fated, in part, by T cell-mediated autoimmunity. Adiponectin (APN) and associated adipokines were shown to be immune tolerance inducers, although the clinically relevant delivery method into target pathologies is under debate. Whether the cell sheet-based delivery system of adipokines might induce immune tolerance and functional recovery in experimental autoimmune myocarditis (EAM) was tested.

**Methods and Results:** Scaffold-free-induced adipocyte cell-sheet (iACS) was generated by differentiating adipose tissue-derived syngeneic stromal vascular-fraction cells into adipocytes on temperature-responsive dishes. Rats with EAM underwent iACS implantation or sham operation. Supernatants of iACS contained a high level of APN and hepatocyte growth factor (HGF), and reduced proliferation of CD4-positive T cells in vitro. Immunohistolabelling showed that the iACS implantation elevated the levels of APN and HGF in the myocardium compared to the sham operation, which attenuated the immunological response by inhibiting CD68-positive macrophages and CD4-positive T-cells and activating Foxp3-positive regulatory T cells. Consequently, left ventricular ejection fraction was significantly greater after the iACS implantation than after the sham operation, in association with less collagen accumulation.

**Conclusions:** The targeted delivery of adipokines using tissue-engineered iACS ameliorated cardiac performance of the EAM rat model via effector T cell suppression and induction of immune tolerance. These findings might suggest a potential of this tissue-engineered drug delivery system in treating fulminant myocarditis in the clinical setting. (*Circ J* 2015; **79**: 169–179)

**Key Words:** Adiponectin; Inflammation; Myocarditis; Transplantation

Fulminant myocarditis often follows a rapidly deteriorating course, leading to severe cardiac dysfunction. Efficacy of fast-track immunoglobulin and steroid therapies has been reported,<sup>1</sup> but these treatments are not fully established. Although the pathogenesis of fulminant myocarditis is not fully understood, an autoimmune response against myocardial components has been suggested to play an important role in its progression, consequently leading to end-stage heart failure.<sup>1,2</sup> Interferon (IFN) $\gamma$ -producing T helper (Th)1 cells and interleukin (IL)17-producing Th17 cells are reported to be key regulators of the autoimmune response, as they ac-

tivate macrophages in the cardiac tissues to trigger inflammation and inhibit regulatory T cells.<sup>2,3</sup> Strategies for ameliorating the immune response and/or augmenting immune tolerance are therefore under development for treating fulminant myocarditis.

### Editorial p51

Fat tissue functions as a type of endocrine organ by secreting its produced cytokines and adipokines, which have pro-inflammatory and anti-inflammatory activities. Adiponectin

Received July 31, 2014; revised manuscript received September 13, 2014; accepted September 24, 2014; released online November 5, 2014 Time for primary review: 19 days

Department of Cardiovascular Surgery (S.K., S.M., S.F., Y.I., A.S., Y.S.), Department of Metabolic Medicine (N.M., I.S.), Osaka University Graduate School of Medicine, Suita, Japan

Mailing address: Yoshiki Sawa, MD, PhD, Department of Cardiovascular Surgery, Osaka University Graduate School of Medicine, 2-2 Yamadaoka, Suita 565-0871, Japan. E-mail: sawa-p@surg1.med.osaka-u.ac.jp

ISSN-1346-9843 doi:10.1253/circj.CJ-14-0840

All rights are reserved to the Japanese Circulation Society. For permissions, please e-mail: [cj@j-circ.or.jp](mailto:cj@j-circ.or.jp)



(APN) is an adipokine with strong anti-inflammatory properties and has been suggested to play a protective role in the acute phase of myocarditis in humans.<sup>4,5</sup> Importantly, it has been known that APN is downregulated in a variety of clinical conditions or critical illnesses, such as obesity, type 2 diabetes, and coronary artery disease.<sup>6</sup> In addition, hepatocyte growth factor (HGF), another known anti-inflammatory adipokine, was reported to induce immune tolerance and functional recovery by use of an *in vivo* transfection technique in experimental autoimmune myocarditis (EAM).<sup>7,8</sup> However, no clinically relevant method for the efficient delivery of APN or HGF into the heart has been well established for treating fulminant myocarditis.

We previously developed the epicardial transplantation of scaffold-free-induced adipocyte cell-sheet (iACS) method, and recently showed that iACS can constitutively deliver a variety of cardioprotective factors, including APN and HGF, to the heart in mice subjected to acute myocardial infarction.<sup>9</sup> Importantly, iACS is generated from adipose tissue-derived stromal vascular fraction (SVF) cells that are isolated from the subcutaneous fat tissue without gene modification, which is promising for the potential use of this method in clinical settings.

We hypothesized that iACS transplantation into the heart might induce immune tolerance and functional recovery in autoimmune-associated myocarditis. Here we examined the biological and functional effects of this method as a drug-delivery system using an EAM rat model. Immunoinhibitory effects of pivotal paracrine factors, such as APN and HGF, on dendritic and effector T cells were also analyzed *in vivo* and *in vitro*. In addition, we generated a non-differentiating SVF cell-sheet (SVFCS) and showed that both the iACS and SVFCS produce a similarly great amount of anti-inflammatory adipokines, including HGF; however, differentiated iACS but not SVFCS was able to secrete a large amount of APN. Therefore, for the purpose of examining the additional effect of APN on EAM, we compared the therapeutic effects of iACS implantation with those of SVFCS implantation.

## Methods

### Animals

All animal studies were carried out under approval of the institutional ethics committee. This investigation conforms to the Principles of Laboratory Animal Care formulated by the National Society for Medical Research and the Guide for the Care and Use of Laboratory Animals (US National Institutes of Health Publication No. 85-23, revised 1996).

### Preparation of SVFCS and iACS

Each iACS was prepared as previously described.<sup>9</sup> Briefly, SVF cells isolated from inguinal adipose tissue were cultured on 35-mm thermo-responsive dishes (CellSeed, Tokyo, Japan), at  $2 \times 10^6$  cells per dish, to generate each scaffold-free SVFCS. Each iACS was generated by adding 10 mg/ml insulin, 2 mmol/L dexamethasone, 5 mmol/L pioglitazone, and 125 mmol/L isobutylmethylxanthine (Sigma-Aldrich, St Louis, MO, USA) to the SVFCS for 2 days. The medium was then refreshed and the cultures incubated for 5 more days at 37°C. The iACS spontaneously detached from the surface when placed in a 20°C refrigerator.

### Generation of the Rat Myocarditis Model and Cell-Sheet Transplantation

Purified porcine cardiac myosin (Sigma-Aldrich) was dis-

solved in 0.01 mol/L phosphate-buffered saline and emulsified with an equal volume of complete Freund's adjuvant (Difco Laboratories, Detroit, MI, USA). On days 0 and 7, 0.2 ml of the emulsion, which yielded an immunizing dose of 1.0 mg cardiac myosin per rat, was injected subcutaneously into the footpad of male Lewis rats (7 weeks old, 200–250 g).<sup>2</sup> Following the second injection, the rats were randomly assigned to 3 groups and subjected to a thoracotomy and: (1) a sham operation (Sham group;  $n=58$ ) or transplantation onto the anterior surface of the heart of; (2) 3-layered SVFCS (SVFCS group;  $n=54$ ); or (3) 3-layered iACS (iACS group;  $n=58$ ).

### Echocardiography and Conductance Catheter

Serial transthoracic echocardiography was performed under inhaled anesthesia with isoflurane (1.5%, 1 L/min; Mylan, Pittsburgh, PA, USA). Two-dimensional short-axis images at the basal, mid, and apical levels were acquired to calculate the left ventricular (LV) ejection fraction (EF) and regional wall motion index (RWMI).<sup>10</sup>

Pressure-volume (P-V) cardiac catheterization was performed after median sternotomy, by inserting a conductance catheter (Unique Medical, Tokyo, Japan) and a Micro Tip catheter transducer (SPR-671; Millar Instrument, Houston, TX, USA) into the LV cavity. The P-V loop data under stable hemodynamics or inferior vena cava occlusion were analyzed with Integral 3 software (Unique Medical).

### CD4-Positive T-Cell Proliferation Assay

CD4-positive T cells and antigen-presenting dendritic cells were isolated from the spleen of EAM and normal rats, respectively, using magnetic-bead systems (Miltenyi Biotec, Bergish Gladbach, Germany). The isolated CD4-positive T cells and antigen-presenting dendritic cells were co-cultured in RPMI 1640 (Gibco, Grand Island, NY, USA) and 10% fetal bovine serum (FBS), supplemented with iACS supernatant, recombinant APN (Adipo Bioscience, CA, USA), or recombinant HGF (Institute of Immunology, Tokyo, Japan) for 5 days. Subsequently, 50 µg/ml purified porcine heart myosin was added, and T-cell proliferation was estimated using the Cell Counting Kit-8 (Dojindo, Kumamoto, Japan).<sup>8</sup>

### Histology

Myocarditis severity was graded on hematoxylin and eosin (H&E)-stained whole sections (0, no inflammatory infiltrates; 1, small foci of inflammatory cells; 2, larger foci <100 inflammatory cells; 3, more than 10% of a cross-section involved; and 4, more than 30% of a cross-section involved).<sup>11</sup> The CD68-, CD4-, or CD4/Foxp3-positive cells were counted in 5 random fields (magnification:  $\times 600$ ) to assess the infiltration of macrophages, CD4-positive T cells, or Foxp3-positive regulatory T cells, respectively.<sup>8</sup>

### Statistical Analysis

Values are given as the mean  $\pm$  SD. All analyses were performed using SPSS 11.0J for Windows (SPSS, Chicago, IL, USA) and the R program.

Detailed methods are presented in [Supplementary File 1](#).<sup>9</sup>

## Results

### Characterization of SVFCS and iACS *In Vitro*

The characteristics and fundamental behavior of the SVFCS and iACS were compared histologically and biochemically *in vitro*. The cells in the SVFCS were confluent and spindle-shaped. The cells in iACS were similar but many contained a



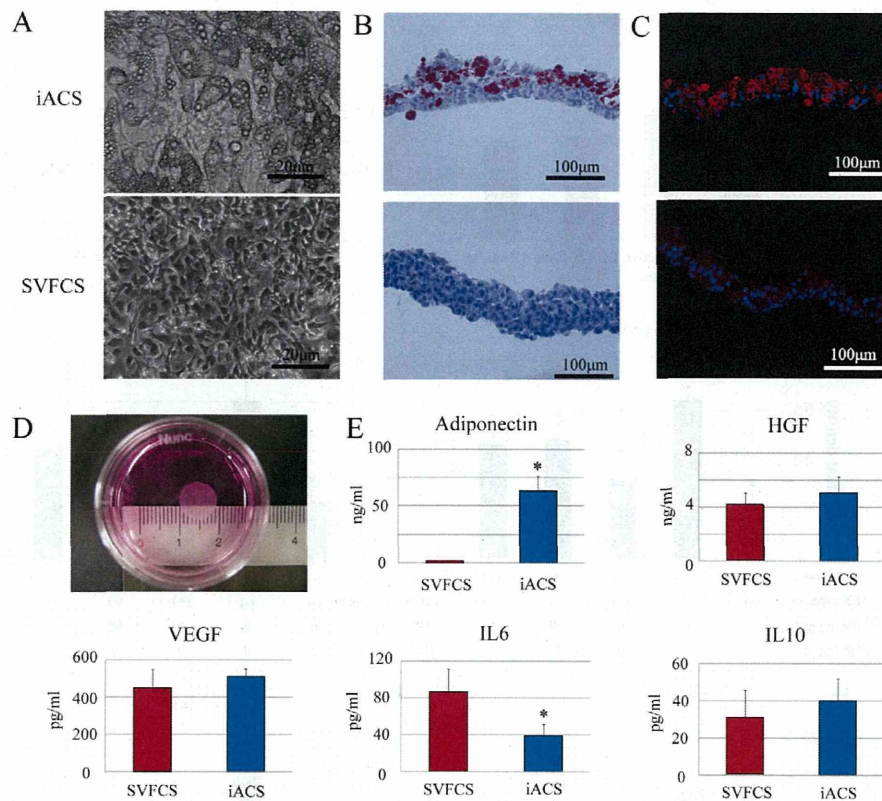


**Figure 1.** Characterization of the induced adipocyte cell sheet (iACS) in vitro. (A) Representative micrographs (B) Oil-red O staining. (C) Representative immunostaining for adiponectin (APN). Red indicates APN; blue, nuclei (n=7 each). (D) iACS detached from the temperature-responsive culture dish. (E) APN, hepatocyte growth factor (HGF), vascular endothelial growth factor (VEGF), interleukin (IL)6, and IL10 cytokine levels in cell-sheet supernatants by ELISA analysis (n=7 each). \* $P<0.05$  vs. stromal vascular fraction cell-sheet (SVFCS). There was significantly more released APN in the culture supernatant of iACS than of SVFCS ( $P<0.001$ , unpaired t-test).

number of small cytoplasmic vesicles (Figure 1A) that stained positive with oil-red O, indicating that the vesicles were fat droplets. Only approximately half the SVF cells had differentiated into adipocytes (Figure 1B). Each iACS was approximately 9 mm in diameter and 140- $\mu$ m thick (Figure 1D). Immunohistolabeling revealed that APN was markedly upregulated in the cytoplasm of mature adipocytes in the iACS, but not in the undifferentiated SVF cells in the SVFCS (Figure 1C). The amount of extracellularly released APN in vitro was significantly and markedly greater in the culture supernatant of the iACS than in that of the SVFCS ( $P<0.001$ ), as assessed by enzyme-linked immunosorbent assay (ELISA) (Figure 1E). The levels of HGF, vascular endothelial growth factor (VEGF) and anti-inflammatory IL10 were not significantly different between the SVFCS and the iACS, whereas the level of pro-inflammatory IL6 in the iACS culture supernatant was significantly lower ( $P=0.001$ ).

#### Inhibition of Antigen-Specific CD4-Positive T-Cell Proliferation by iACS In Vitro

We first examined the expression of 2 different APN receptors (AdipoR1 and AdipoR2) in CD4-positive T cells, CD8-positive T cells and dendritic cells. Using quantitative real-time PCR, we detected similar levels of 2 genes in these 3 cell types

(Figure 2A).

Next, the effects of iACS transplantation on CD4-positive T-cell-related immunity in the EAM rats were assessed by an antigen-specific T-cell proliferation assay in vitro.

The addition of porcine myosin significantly and markedly increased the proliferation of CD4-positive T cells that were isolated from the spleen of the EAM rats (Figure 2B). The addition of recombinant APN and HGF at more than 30 ng/ml and 2 ng/ml, respectively, significantly suppressed the antigen-induced CD4-positive T-cell proliferation (Figure S1). The proliferation was diminished significantly more by the addition of an iACS supernatant, compared with 60 ng/ml APN or 5 ng/ml HGF, which were the average amounts released by iACS in vitro ( $P<0.001$  for Myosin (+) vs. APN (60 ng/ml) and HGF (5 ng/ml vs. iACS supernatant). VEGF addition did not have any effect on T-cell proliferation (data not shown). ELISA analysis of the supernatant after incubating the antigen-induced CD4-positive T cells with a specific antigen revealed that adding recombinant APN (60 ng/ml), recombinant HGF (5 ng/ml) or iACS supernatant significantly diminished the release of IFN $\gamma$ , IL17 and IL6 from the cells (Figures 2C–E).



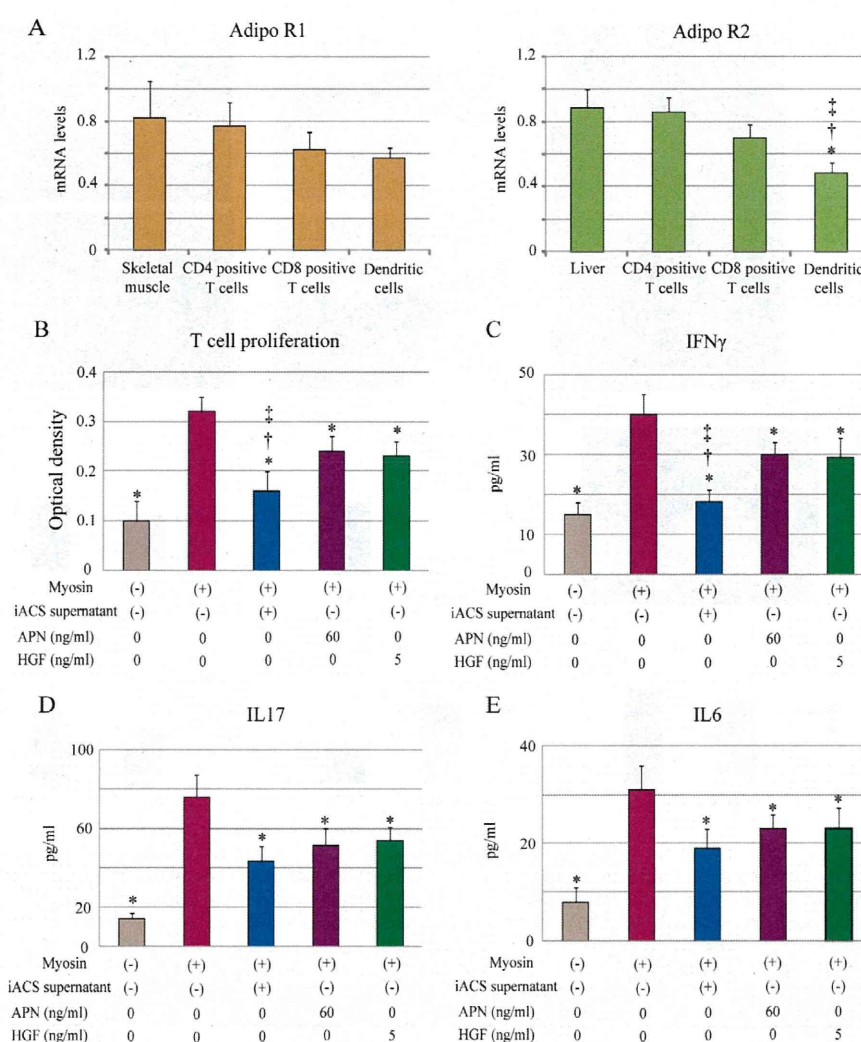


**Figure 2.** Expression of adiponectin (APN) receptors and CD4-positive T-cell proliferation assay. **(A)** mRNA levels of 2 different APN receptors (AdipoR1 and AdipoR2) in CD4-positive T cells, CD8-positive T cells and dendritic cells ( $n=7$  each, ANOVA). \* $P<0.05$  vs. Liver, † $P<0.05$  vs. CD4 positive T cells, ‡ $P<0.05$  vs. CD8 positive T cells. All mRNA levels are normalized to GAPDH. **(B–E)** Addition of induced adipocyte cell-sheet (iACS) supernatant, recombinant APN (60 ng/ml) or hepatocyte growth factor (HGF) (5 ng/ml) significantly suppressed the CD4-positive T-cell proliferation ( $P<0.001$ ) and production of interferon (IFN) $\gamma$  ( $P<0.001$ ), interleukin (IL)17 ( $P<0.001$ ) and IL6 ( $P<0.001$ ) ( $n=7$  each, ANOVA). \* $P<0.05$  vs. Myosin (+), † $P<0.05$  vs. APN (60 ng/ml), ‡ $P<0.05$  vs. HGF (5 ng/ml).

### Delivery of APN, HGF and VEGF Into EAM Rat Heart by iACS Transplantation

The expression of APN, HGF and VEGF in the EAM rat heart after treatment was assessed by immunohistolabeling and ELISA. Most of the green fluorescent protein (GFP)-positive transplanted cells on day 21 in both the SVFCS and iACS groups remained on the surface of the heart (Figures 3B,C), and the number in both engrafted cell sheets gradually decreased from day 8 to day 42 (SVFCS:  $P=0.026$ , iACS:  $P=0.045$ ; Figure 3J). Relatively small amounts of APN were detected at the inflamed interstitium and perivascular area in the Sham and SVFCS groups on day 21 (Figures 3A,B). In the iACS group, APN expression was higher at the interstitium near the inflammatory cells and the perivascular area,

especially in the epicardium near the transplanted iACS.

ELISA showed that the cardiac expression of APN in the inflamed area gradually increased over 42 days in the Sham and SVFCS groups, whereas the iACS transplantation significantly and markedly increased the APN expression compared to the other groups for 21 days; thereafter, high APN expression was maintained through the 42 days of the experiment (APN on day 21:  $P=0.007$  for iACS vs. SVFCS and Sham; Figure 3G). Both HGF and VEGF were expressed in the inflamed area, but not in the non-inflamed area, on day 21 as assessed by immunohistolabeling (data not shown); the expression levels of HGF and VEGF on days 21 and 42 were similarly greater in the SVFCS and iACS groups than in the Sham group (HGF on day 21:  $P=0.001$  for iACS and SVFCS



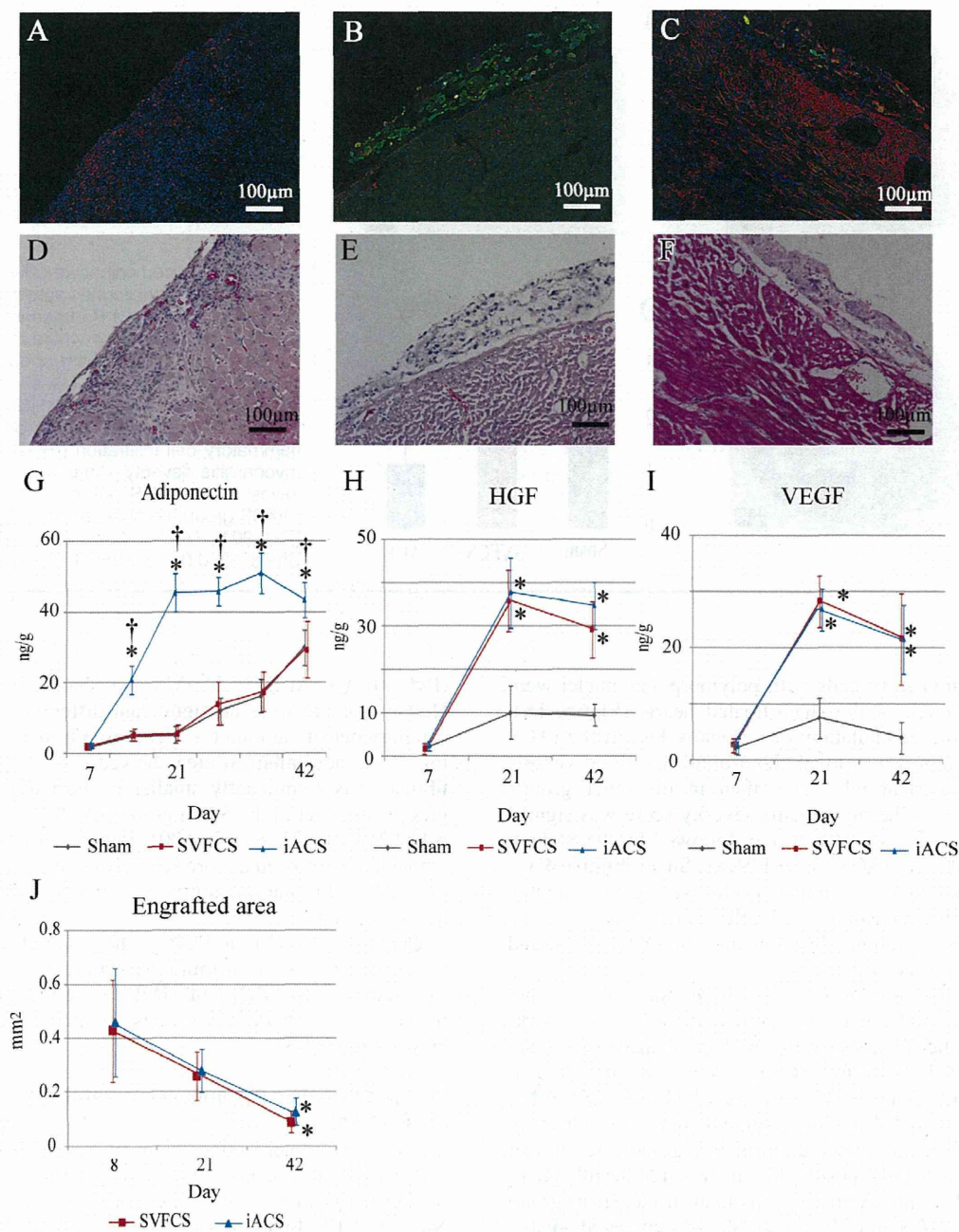


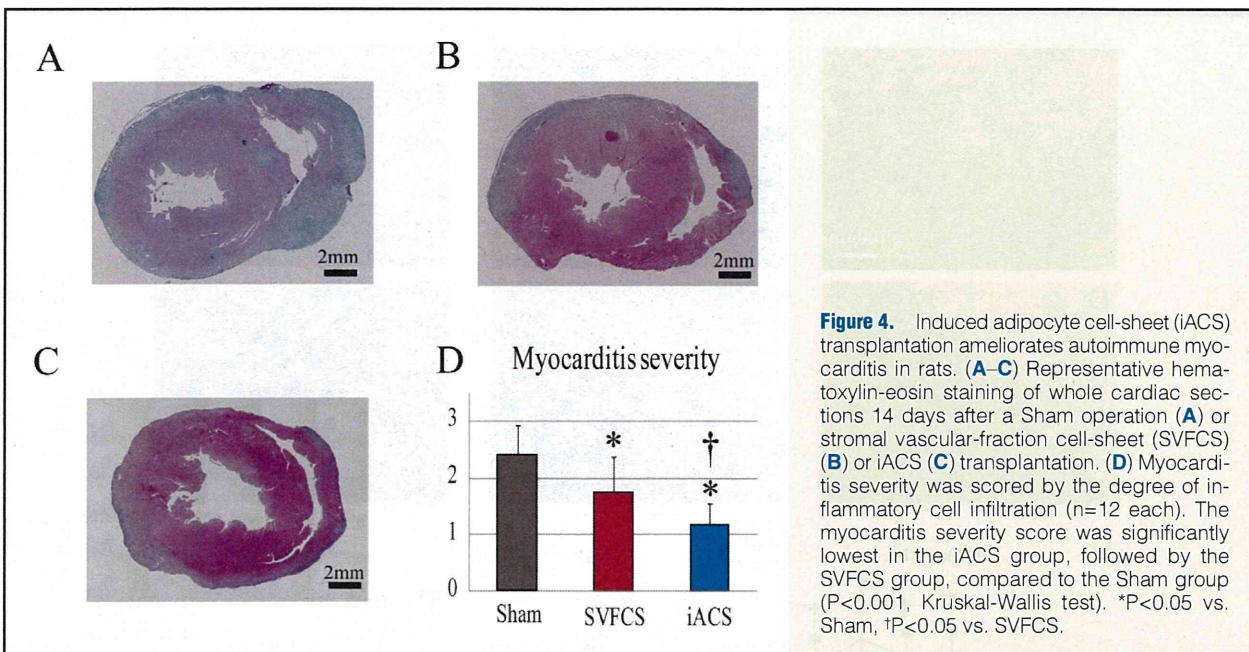
**Figure 3.** Delivery of cardioprotective factors to the experimental autoimmune myocarditis (EAM) rat heart by induced adipocyte cell-sheet (iACS) transplantation in vivo. (A–C) Representative immunostaining for adiponectin (APN) 14 days after the Sham operation (A), or green fluorescent protein (GFP)-positive stromal vascular-fraction cell-sheet (SVFCS) (B) and iACS (C) transplantation, respectively. Red, APN; blue, nuclei. (D–F) Hematoxylin and eosin staining of a serial section from the sample in (A), (B) and (C), respectively. (G–I) Cardiac expression of APN (G), hepatocyte growth factor (HGF) (H), and vascular endothelial growth factor (VEGF) (I) over time by ELISA (APN: Sham, n=7; SVFCS, n=6; iACS, n=7) (HGF and VEGF: Sham, n=6; SVFCS, n=5; iACS, n=7). \*P<0.05 vs. Sham, †P<0.05 vs. SVFCS. (J), Quantification of the engrafted GFP-positive cell-sheet area in the iACS and SVFCS groups (n=4 each). \*P<0.05 vs. day8.

vs. Sham] [VEGF on day 21: P<0.001 for iACS and SVFCS vs. Sham]) (Figures 3H,I).

**Induced ACS Transplantation Ameliorates Autoimmune Myocarditis in Rats**

The severity of myocarditis in the EAM rats on day 21 was assessed and scored using H&E-stained heart sections (n=12





each).<sup>10</sup> Inflammatory cells with polymorphous nuclei were abundant throughout the sham-treated hearts (Figure 4A). The degree of accumulation was globally less in the iACS group, in which it was localized around the blood vessels or near the pericardial tissue, than in the other groups (Figures 4B,C). The myocarditis severity score was significantly smallest in the iACS group, followed by the SVFCS group ( $P=0.001$  for iACS vs. SVFCS vs. Sham; Figure 4D).

The distribution of accumulated cells that regulate immune reactions, such as macrophages, T cells, and regulatory T cells, was evaluated by immunohistolabeling for CD68, CD4, and CD4/Foxp3, respectively.

The accumulation of CD68-positive macrophages and CD4-positive T cells in the myocardial interstitium was markedly and significantly lower in the iACS group than in the Sham group ([CD68:  $P<0.001$  for iACS vs. SVFCS vs. Sham] [CD4:  $P<0.001$  vs. iACS and SVFCS vs. Sham]) (Figures 5A,B,D). Although Foxp3/CD4-double positive regulatory T cells were not abundant in the myocardium of any group, the ratio of Foxp3-positive to CD4-positive T cells was significantly greater in the iACS and SVFCS groups than in the Sham group ( $P=0.006$  for iACS and SVFCS vs. Sham; Figures 5C–E).

The levels of molecules that regulate immune reactions or inflammation, such as IFN $\gamma$ , monocyte chemoattractant protein (MCP)1, tumor necrosis factor (TNF) $\alpha$ , and IL17, in the heart tissue, were significantly lower in the iACS and the SVFCS groups compared to the Sham group, as assessed by using an ELISA (Figure 5F).

#### Reverse LV Remodeling by iACS Transplantation in EAM Rats

Typical histological features of LV remodeling, such as myocyte hypertrophy, capillary density and collagen accumulation, were assessed in the LV of the EAM rats by using H&E staining, immunohistolabeling for CD31, and Masson-trichrome (MT) staining, respectively. On day 42, H&E staining revealed that the myocyte diameter was significantly smaller in the iACS group than in the SVFCS and Sham groups

( $P<0.001$  for iACS vs. SVFCS and Sham) (Figures 6A,C). However, there were no significant differences in vascular-capillary density among the 3 groups (Figure S2). MT staining of the non-inflamed area showed that the percentage of fibrosis was significantly smaller in the iACS and SVFCS groups than that in the Sham group (iACS,  $4.5\pm 2.1$ ; SVFCS,  $6.1\pm 2.2$ ; Sham,  $21\pm 6\%$ ;  $P<0.001$ ; Figures 6B,D). MT-stained whole hearts showed a more severely enlarged LV cavity and thin LV wall in the Sham group compared with the iACS or SVFCS groups.

Quantitative real-time PCR of these samples showed that the expressions of transforming growth factor (TGF) $\beta$ , metalloproteinases (MMP)2, and MMP9 were significantly lower in the iACS and SVFCS groups compared with the Sham group (Figure S3).

#### Preserved Cardiac Performance by iACS Transplantation in the EAM Rats

Cardiac performance after treatment was evaluated by serial echocardiography every 7 days and by cardiac catheterization on day 42. The hearts of all the groups showed gradually decreased LVEF (Figure 7A) and increased RWMI (Figure 7B) until day 56. However, the progressive changes in LVEF and RWMI were significantly least severe in the iACS group, followed by the SVFCS group, and then the Sham group (LVEF on day 56: iACS,  $56.7\pm 5.0$ ; SVFCS,  $46.9\pm 7.2$ ; Sham,  $35.3\pm 5.0\%$ ;  $P<0.001$  for iACS vs. SVFCS vs. Sham). The hearts of all the groups showed a gradually decreased LV anterior wall diameter (AWD) and enlarged LV end-diastolic dimension (EDD) until day 56. Both LVAWD and LVEDD on day 42 were significantly larger and smaller, respectively, in the iACS and SVFCS groups than in the Sham group (Figures 7C,D; LVAWD:  $P<0.001$  for iACS and SVFCS vs. Sham; LVEDD:  $P<0.001$  for iACS and SVFCS vs. Sham). Cardiac catheterization using a conductance catheter revealed that the end-systolic pressure-volume relationship (ESPVR) was significantly greater in the iACS group than in the Sham group ( $P<0.001$  for iACS vs. SVFCS vs. Sham; Figure 7E).



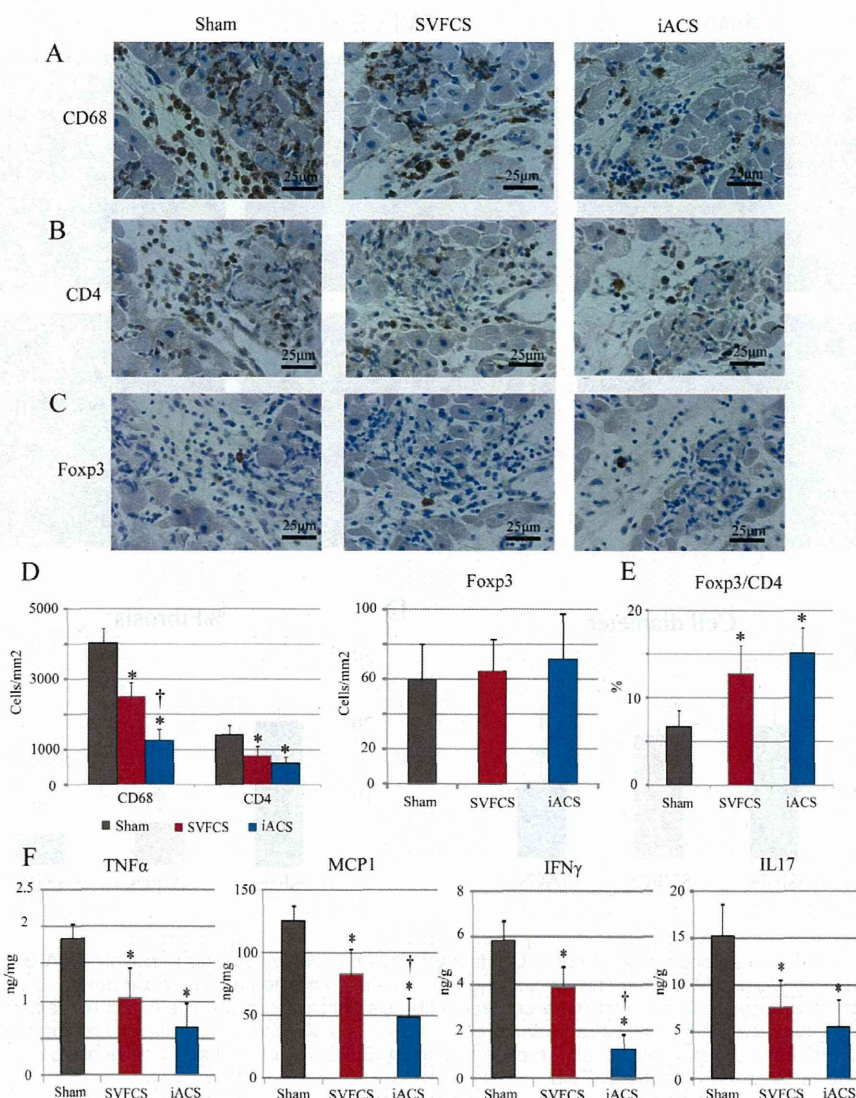


**Figure 5.** Induced adipocyte cell-sheet (iACS) suppressed the effector T-cell and macrophage responses, and promoted the regulatory T-cell response in experimental autoimmune myocarditis (EAM) rat heart. (**A–C**) Representative immunostaining for CD68 (**A**), CD4 (**B**), and Foxp3 (**C**) on postoperative day 14 in each group. (**D**) Quantification of CD68, CD4, and CD4/Foxp3-positive cells (n=12 each). CD68-positive macrophage accumulation in the myocardial interstitium was lowest in the iACS group followed by the stromal vascular-fraction cell-sheet (SVFCS) group compared to the Sham group ( $P<0.001$ , ANOVA). \* $P<0.05$  vs. Sham, † $P<0.05$  vs. SVFCS. (**E**) Ratio of Foxp3-positive regulatory cells to CD4-positive T cells. \* $P<0.05$  vs. Sham (n=12 each). (**F**) Myocardial tissues of EAM rat were homogenized and subjected to ELISA to detect tumor necrosis factor (TNF) $\alpha$ , monocyte chemoattractant protein (MCP)1, interleukin (IL)17, and interferon (IFN) $\gamma$  (n=12 each). \* $P<0.05$  vs. Sham, † $P<0.05$  vs. SVFCS.

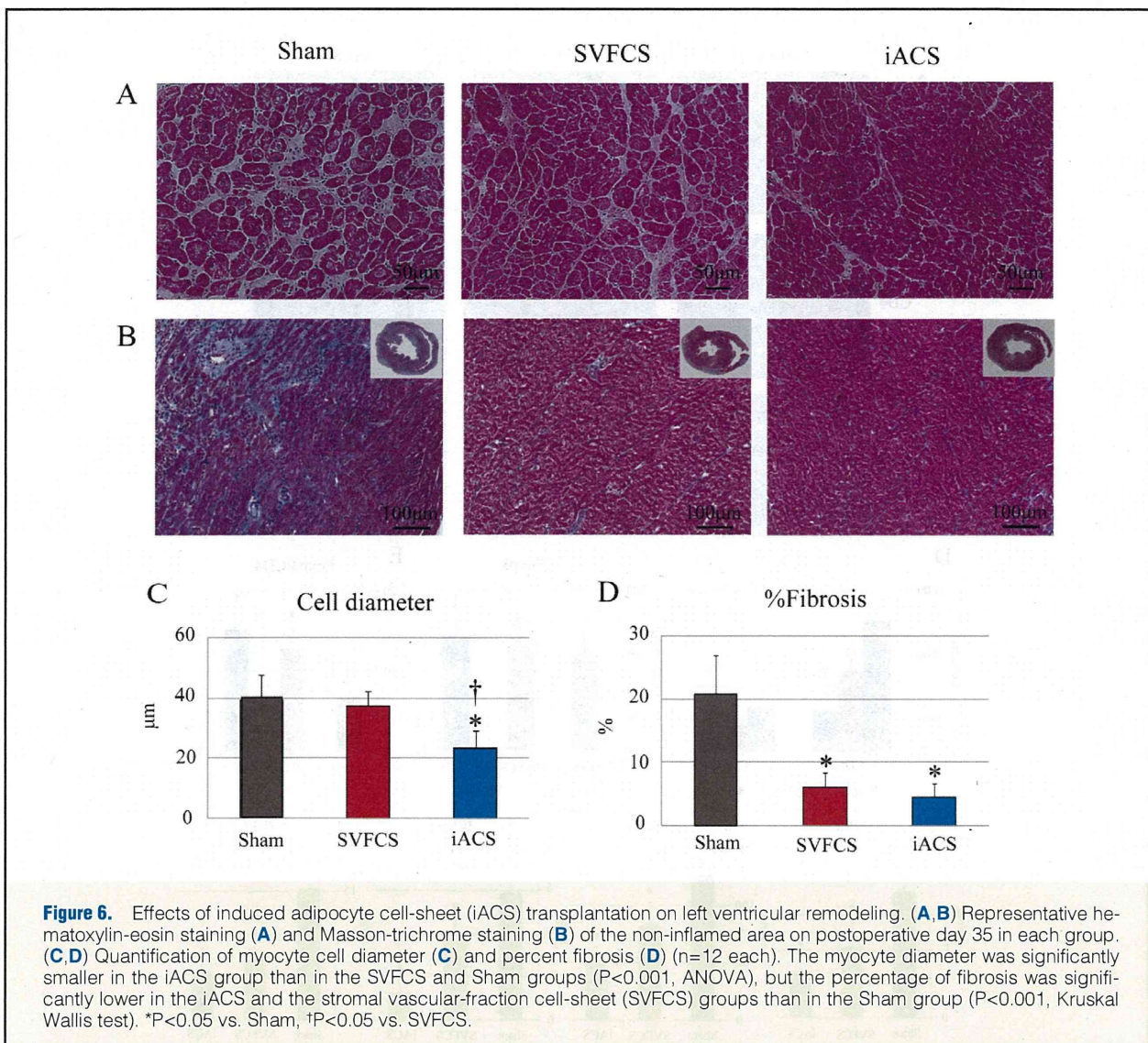
In addition, both  $dP/dt$  max and  $-dP/dt$  min were significantly greater in the iACS group than in the other groups (Table S1).

## Discussion

We demonstrated here that iACS, which is generated from SVF isolated from subcutaneous fat tissues, extracellularly released a variety of cardioprotective factors including APN in vitro, and the released factors efficiently inhibited antigen-specific T-cell proliferation via the downregulation of IFN $\gamma$ , IL17, and IL6 in vitro. Epicardially transplanted iACS sup-

plied greater amounts of cardioprotective factors, such as APN, HGF or VEGF, into the inflamed myocardium of EAM rat hearts for at least 35 days, compared to the SVFCS transplantation or the Sham operation. Consequently, the iACS-transplanted EAM rat hearts showed less severe inflammation, lower expression levels of inflammatory cytokines, and a greater Foxp3-positive regulatory T-cell ratio, compared to the SVFCS-transplanted or Sham-operated EAM hearts. In addition, there was less progression of histological and functional LV remodeling in the EAM hearts following the iACS transplantation than after SVFCS transplantation or the Sham op-





eration.

Fat tissue is known to play a variety of important biological and physiological roles.<sup>12,13</sup> While bloated and/or degenerated fat tissues release inflammatory and atherogenic factors, intact normal fat tissues release protective factors represented by APN, which have anti-inflammatory/apoptotic/fibrotic effects on a variety of cardiac pathologies.<sup>12–14</sup> Importantly, protective factors, including APN, have been shown to be released by mature adipocytes, but not by undifferentiated ones such as SVF cells.<sup>9</sup> Because the cell culture of freshly isolated mature adipocytes and cell-sheet generation from these cells are technically difficult, we generated cell sheets containing mature adipocytes by inducing the cells in SVFCS to differentiate in vitro. We confirmed that both the iACS and SVFCS released little inflammation-related or atherogenic adipokines in vitro. In contrast, differentiated iACS but not SVFCS could secrete a large amount of APN.

Although the lifespan of adipocytes is generally shorter than that of SVF cells, SVF cells are known to appropriately and autonomously differentiate into adipocytes in vivo in adipose

tissues in response to increased adipocyte cell death. Considering this reciprocal regulation between the 2 cell types, we ascertained that a minimum, rather than maximum, induction of differentiation might allow the iACS to provide APN to the host myocardium for a long time. In fact, iACS contained a certain amount of undifferentiated SVF cells before transplantation. While iACS supplied significantly more APN to EAM hearts than did SVFCS, the APN level in the inflamed myocardium was not different between the SVFCS-transplanted and Sham-operated hearts, suggesting that SVFCS did not release substantial APN after its transplantation into the heart. This contrary effect that SVF cells could differentiate into mature adipocytes in vitro, but not in vivo, could be explained by the different conditions for the differentiation from SVF cells to mature adipocytes. The appropriate induction of differentiation to iACS in vitro might have maintained the normal capacity of the adipocytes and/or SVF cells in the sheet to release abundant APN or other protective factors after transplantation, thereby eliciting the substantial therapeutic effects noted in this study.



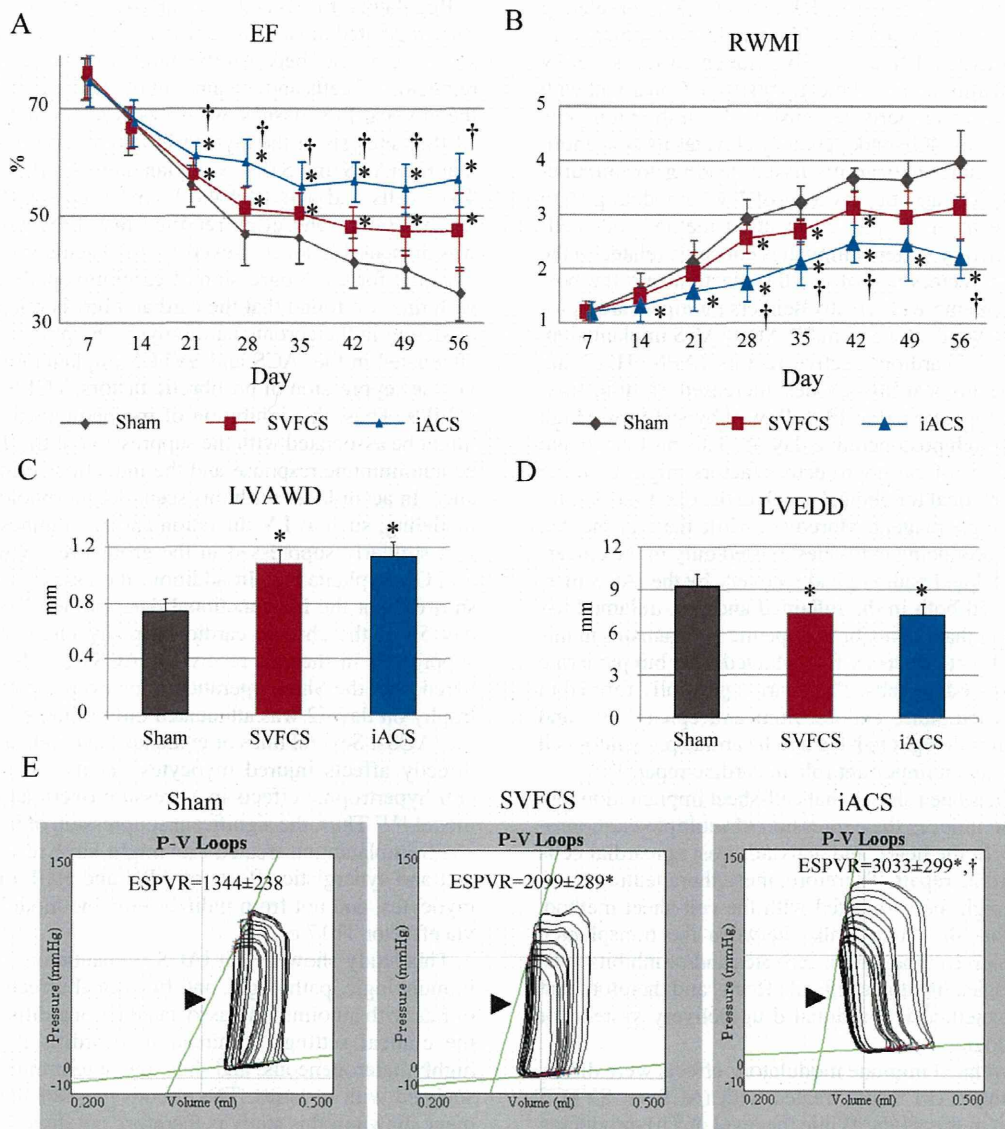


**Figure 7.** Cardiac structure and function after induced adipocyte cell-sheet (iACS) transplantation. (**A,B**) Serial echocardiographic parameters (**A**, ejection fraction [EF], **B**, regional wall motion index [RWMI]) in each group (day 7–day 42,  $n=12$  each; day 49–day 56,  $n=6$  each). The left ventricular (LV) EF was greatest in the iACS group, followed by the stromal vascular-fraction cell-sheet (SVFCS) group, then the Sham group ( $P<0.001$ , ANOVA). \* $P<0.05$  vs. Sham, † $P<0.05$  vs. SVFCS. (**C,D**) LV anterior wall diameter (LVAWD) (**C**) and end-diastolic diameter (LVEDD) (**D**) on day 42 ( $n=12$  each). LVEDD on day 42 was significantly lower in the iACS and SVFCS groups than in the Sham group ( $P<0.001$ , Kruskal-Wallis test). \* $P<0.05$  vs. Sham. (**E**) Representative pressure-volume (P-V) loops on day 42 from each group ( $n=7$  in each). Slopes indicate the end-systolic P-V relationship (ESPVR) (arrows). Representative P-V loops during inferior vena cava occlusion showed that the ESPVR was significantly greater in the iACS group than in the other groups ( $P<0.001$ , ANOVA). \* $P<0.05$  vs. Sham, † $P<0.05$  vs. SVFCS.

The transplantation of either SVFCS or iACS resulted in positive pathological and functional effects on the EAM hearts in this study, although the impact was greater following iACS transplantation. The findings indicate that APN, which was more substantially increased in the iACS-transplanted hearts than in the SVFCS-transplanted ones, was a key factor accounting for the difference between the iACS and SVFCS treatments.<sup>7</sup> HGF and/or VEGF, which were increased in both

the iACS and the SVFCS groups, have also been suggested to elicit therapeutic effects.<sup>8</sup>

Importantly, following iACS transplantation, both APN and HGF were present near CD4-positive effector T cells, which are known to express APN and HGF receptors,<sup>7,8</sup> suggesting that the upregulated APN and HGF might inhibit the accumulation of effector T cells and macrophages, and promote the accumulation of Foxp3 regulatory T cells, consequently at-